

Seasonal prediction of the typhoon genesis frequency over the Western North Pacific with a Poisson regression model

Xinchang Zhang¹ · Shanshan Zhong¹ · Zhiwei Wu² · Yun Li³

Received: 23 June 2016 / Accepted: 20 March 2017
© Springer-Verlag Berlin Heidelberg 2017

Abstract This study investigates the typhoon genesis frequency (TGF) in the dominant season (July to October) in Western North Pacific (WNP) using observed data in 1965–2015. Of particular interest is the predictability of the TGF and associated pre-season sea surface temperature (SST) in the Pacific. It is found that, the TGF is positively related to a tri-polar pattern of April SST anomalies in North Pacific (NPT_{Apr}), while it is negatively related to SST anomalies over the Coral Sea ($CSST_{Apr}$) off east coast of Australia. The NPT_{Apr} leads to large anomalous cyclonic circulation over North Pacific. The anomalous southwesterly weakens the northeast trade wind, decreases evaporation, and induces warm water in central tropical North Pacific. As such, the warming effect amplifies the temperature gradient in central tropical North Pacific, which in turn

maintains the cyclonic wind anomaly in the west tropical Pacific, which favors the typhoon genesis in WNP. In the South Pacific, the $CSST_{Apr}$ supports the typhoon formation over the WNP by (a) strengthening the cross-equatorial flows and enhancing the Inter-tropical Convergence Zone; (b) weakening southeast and northeast trade wind, and keeping continuous warming in the center of tropical Pacific. The influence of both NPT_{Apr} and $CSST_{Apr}$ can persistently affect the zonal wind in the tropical Pacific and induce conditions favorable for the typhoon genesis in the typhoon season. A Poisson regression model using NPT_{Apr} and $CSST_{Apr}$ is developed to predict the TGF and a promising skill is achieved.

Keywords Typhoon genesis frequency · Western North Pacific · Prediction · Poisson regression

This paper is a contribution to the special issue on East Asian Climate under Global Warming: Understanding and Projection, consisting of papers from the East Asian Climate (EAC) community and the 13th EAC International Workshop in Beijing, China on 24–25 March 2016, and coordinated by Jianping Li, Huang-Hsiung Hsu, Wei-Chyung Wang, Kyung-Ja Ha, Tim Li, and Akio Kitoh.

✉ Shanshan Zhong
zhongshanshan@nuist.edu.cn

¹ Key Laboratory of Meteorological Disaster, Ministry of Education (KLME), Joint International Research Laboratory of Climate and Environment Change (ILCEC), Collaborative Innovation Center on Forecast and Evaluation of Meteorological Disasters (CIC-FEMD), Nanjing University of Information Science and Technology, Nanjing 210044, China

² Institute of Atmospheric Sciences, Fudan University, Shanghai 200433, China

³ Business Intelligence and Data Analytics, Western Power, Perth 6000, Australia

1 Introduction

The Western North Pacific (WNP) is the most active basin with about 30 TCs (tropical cyclones), including average 16 typhoons per year in the period from 1965 to 2015. The summer-autumn months (JASO, July to October) is the dominant season with 70% typhoons occurring in WNP. It is well-known that WNP typhoons can cause catastrophic destructions to the coastal regions and surrounding areas. For example, Typhoon Megi in 2010 killed 31 people and caused \$255.1 million in damage over Luzon, in the Philippines. It also caused \$42.2 million in damage and killed 38 people in Yilan, Taiwan, and \$411.7 million in damage over Fujian, China. Therefore, it is important to understand the physical processes and build skills of forecasting the typhoon frequency in order to mitigate the impact of the typhoon.

It is known that TC activities depend on thermodynamic factors (e.g., sea surface temperature (SST), mid-tropospheric moisture, and atmospheric instability) and dynamical factors (e.g., the low-level vorticity, vertical wind shear, and upper-tropospheric momentum flux convergence) (Gray 1968, 1979). These factors were widely used in association with the TC genesis research (Chand and Walsh 2010; Li and Zhou 2012). Over the WNP basin prone to frequent TCs, the thermodynamic factors for the TC formation are most favored because the averaged SST is generally above 29°C in the typhoon season (e.g., Wang and Chan 2002), which maintains high temperature and moisture for the generation of TCs. On the other hand, recent studies (e.g., Wang and Chan 2002; Chand and Walsh 2010) demonstrated that local SST anomaly has no obvious relationship with the typhoon activity in WNP. These results suggest that large-scale thermodynamic and dynamical conditions may carry a key responsibility driving the typhoon activity.

The influence of El Niño Southern Oscillation (ENSO) on the TC activity has been investigated in previous studies (e.g., Chan 1985, 1995; Chan et al. 1998, 2001; Chen et al. 1998; Graham and Barnett 1987; Gray 1984; Wang and Chan 2002; Li et al. 2012). It has been demonstrated that the frequency of TC formations over WNP is less than normal in El Niño years, while it tends to be more in La Niña years (Chan 1985, 2000; Dong 1988). Furthermore, Wang and Chan (2002) noticeably forecasted the number of tropical storm formations in southeast and northwest quadrants of the typhoon genesis region during July–December by using preceding winter-spring Niño3.4 SST anomaly. However, as pointed out by many authors (e.g., Chan 1985; Lander and Holland 1993; Ramage and Hori 1981; Wang and Chan 2002), there is no evident relationship between the total number of annual TCs in WNP and ENSO indices. That is, one cannot simply use ENSO indices to predict the frequency of TC formations in the WNP. It remains challenge to found predictors to forecast the frequency of TC (including typhoon) formations in WNP.

Various efforts have been made to understand the predictability of the TC frequency (Li and Zhou 2013a, b, 2014, 2015). Chen et al. (2015) found that boreal spring North Pacific Oscillation (NPO) has a strong correlation ($r = 0.62$) with the annual typhoon number over WNP during the period from 1968 to 2010. They demonstrated that, during a positive phase of spring NPO, the tropical circulation associated with SST anomalies (SSTA) in the North Pacific might result in unfavorable dynamical and thermal conditions for the typhoon genesis over WNP between June and September. As a result, spring NPO may serve as a potential predictor for the frequency of TC formations over WNP. The forcing of the NPO variability is also linked to the boreal spring sea ice in the North Pacific (Fan 2007).

In addition, Zhan et al. (2013) suggested that boreal spring SST gradient (SSTG) between the Southwest Pacific Ocean (40°–20°S, 160°E–170°W) and Western Pacific warm pool (0–16°N, 125°–165°E) might control the interannual variability of the TC frequency over the WNP. They showed that the SSTG could explain 53% of the total variance of the WNP TC frequency during the typhoon season in the period from 1981 to 2011. They further suggested the relationship between the SSTG and WNP TC was an atmospheric response to the SSTG anomalies in boreal spring. Specifically, the positive SSTG anomaly in spring leads to a cross-equatorial pressure gradient, resulting in anomalous southward cross-equatorial flow and tropical easterlies over WNP. The anomalous easterlies further produce the local equatorial upwelling and seasonal cooling in the central Pacific, which in turn maintains the easterly anomalies throughout the typhoon season. As such, the positive SSTG may induce the dynamical/thermodynamical effects (e.g., reduced low-level cyclonic shear, increased vertical wind shear and weakened monsoon trough) that suppress the TC genesis over WNP (Zhan et al. 2013). Zhou and Cui (2011) demonstrated that spring SST off east coast of Australia has a good relationship with the TC frequency in June–October over WNP, which can be considered as a potential predictor of the TC Frequency. Recently, Zhan and Wang (2016) have developed a hybrid dynamical-statistic model to predict the accumulated cyclone energy (ACE) over WNP with four predictors including the above-mentioned factors of April SSTG and SST in southwestern Pacific.

The above researches provide a background that spring SSTA in both Northern and Southern Pacific may act as predictors for forecasting the WNP typhoon frequency in summer and autumn. This motivates us to further investigate the predictors and their associated dynamics for driving the typhoon genesis frequency in the WNP during the typhoon season. Section 2 describes the data and methodology. The climatology of frequency and origins of WNP typhoons are presented in Sect. 3. Results concerning the relationship between spring SST in the Pacific and WNP typhoon frequency are shown in Sect. 4, and the associated mechanisms are discussed in Sect. 5. Section 6 builds a Poisson regression model for forecasting the WNP typhoon genesis frequency (TGF) based on the identified SST predictors. Summary and discussion are given in Sect. 7.

2 Data and methodology

Monthly WNP TGF and typhoon genesis position data were extracted from the typhoon datasets courtesy of Joint Typhoon Warning Center (JTWC) Best Track Data from the website http://weather.unisys.com/hurricane/w_pacific/index.php for the period from 1965 to 2011, and <http://>

weather.unisys.com/hurricane/index.php for the period from 2012 to 2015. A typhoon is defined as a TC with wind speed of 119.1 km/h (74 mi/h) or higher according to the Saffir-Simpson scale standard (Simpson 1974). A typhoon genesis position which is defined as the initial position of the first TC with maximum sustained surface wind equal or greater than 18 m/s.

Monthly wind datasets in the 1965–2015 period were taken from the National Centers for Environmental Prediction-National Center for Atmospheric Research (NCEP-NCAR) reanalysis (Kalnay et al. 1996). The NOAA monthly $2^\circ \times 2^\circ$ extended reconstructed sea surface temperature (ERSST) V3b dataset (Smith and Reynolds 2004) is used to reveal the relationship between TGF and SST (<http://www.ncdc.noaa.gov/ersst/>). The Niño-3.4 index was downloaded from the Climate Prediction Center website http://www.cpc.ncep.noaa.gov/products/analysis_monitoring/ensostuff/detrend.nino34.ascii.txt.

Statistical methods including correlation analysis, principal component analysis (e.g., Li and Smith 2009), partial correlation analysis (e.g., Li et al. 2013; Wu et al. 2015), and Poisson regression (e.g., Cameron and Trivedi 1998), are applied in the paper.

3 Climatology of the TGF

Figure 1a shows the climatological mean of monthly TGF over WNP during the 51-year period from 1965 to 2015. There were 840 typhoons occurring during this period (about 16.5 per year). It is evident that there is a strong seasonal variability in the TGF. In another word, WNP typhoons occur frequently between July and October, accounting for about 72% of the climatological mean annual number of typhoons (11.9 out of 16.5) in 1965–2015. These statistical results are consistent with previous studies (Lander 1994; Yumoto and Matsuura 2001; Chia and Ropelewski 2002). Accordingly, in this study, we focus on investigating the typhoon frequency in the dominant season (JASO).

Figure 1b suggests that the mean positions of typhoon genesis for individual months in JASO are located around the Philippine Sea region centered at (141°E, 16°N). The monthly mean typhoon genesis positions in peak season are within the 29°C isotherm of JASO SST, which reaches its northernmost position, near 17.7°N in August. It is similar to the results of TCs by Chia and Ropelewski (2002), but the typhoon genesis position is at higher latitude and more westward than that of TCs. Because deep convection depends on SST over the threshold of 28°C (Graham and Barnett 1987) and because SST fluctuation in the tropical WNP rarely reaches a strength that brings down the total SST below 28°C in summer (Wang and Chan 2002),

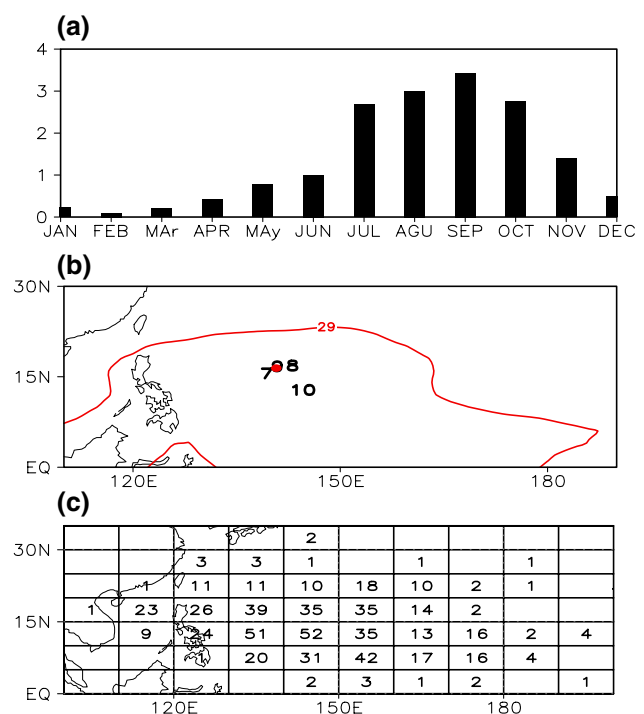
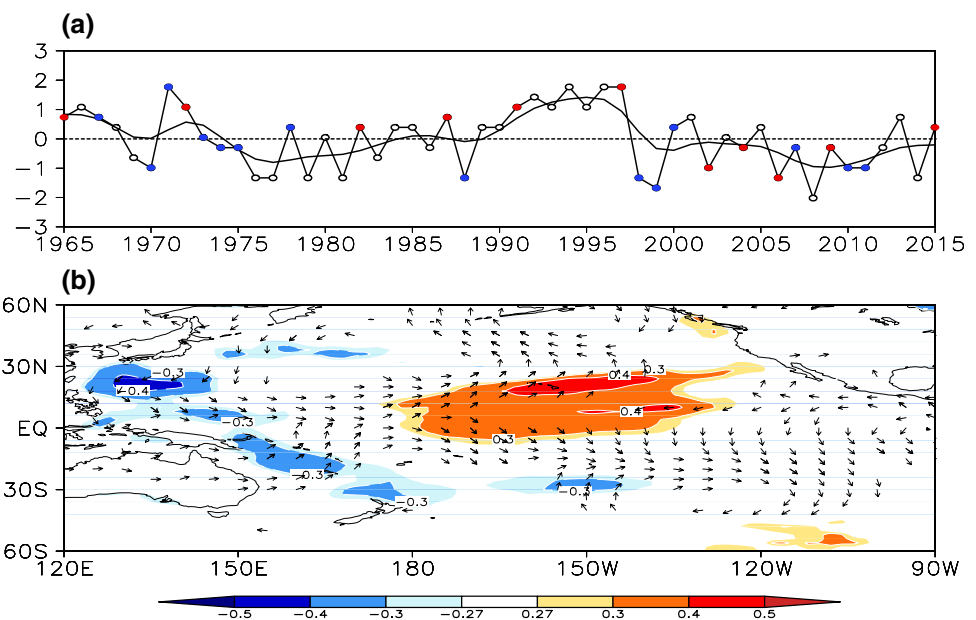


Fig. 1 a The climatological mean of monthly number of WNP typhoons during the period from 1965 to 2015; b Individual mean locations of typhoon genesis positions in months July (7), August (8), September (9) and October (10) in the period between 1965 and 2015. The red point is the average location of all typhoon genesis positions, and the red contour line is the 29°C isotherm of SST in the typhoon season (JASO), 1965–2015. c Spatial distribution of the TGF in typhoon season from 1965 to 2015

Fig. 1b shows that the thermodynamic condition is always satisfied. Thus, the dynamical conditions play a fundamental role in determining the formation of TCs with different intensity. The local SST may influence the TCs intensity. Indeed, as shown in Fig. 1c, the distribution of total number of typhoon formations over WNP in typhoon season during 1965–2015 displays a large spatial variation over much of the 29°C isotherm of JASO SST region. Majority of typhoons occur within the region of (5°–25°N, 110°–180°E), with the largest TGF located at (10°–15°N, 130°–150°E) which is also the center of the area surrounded by 29°C isotherm.

Figure 2a shows the time series of standardized TGF over WNP in JASO during the period from 1965 to 2015. The maximum standardized TGF is 1.77 (equivalent to 17 typhoons), which occurred in 1971, 1994, 1996, 1996, respectively, and the minimum is –2.50 (only six typhoons), happening in 2008. The 8-year smoothed series shows that the frequency is above normal during 1965–1973 and 1989–1997, when the typhoon activity is relatively active; and the frequency is below normal during the periods of 1974–1988 and 1998–2015, when the

Fig. 2 **a** Standardized time series of the TGF in the typhoon season (JASO), 1965–2015. Warm events (*red solid circle*) and cold events (*blue solid circle*) are defined by JASO Niño-3.4 index below /above 0.5 °C. *Solid line* is 8-year smoothed; **b** Correlation between the JASO TGF and SST/850 hPa wind during the period 1965–2015. Significant positive/negative correlations between the TGF and SST at the 0.05 level are marked as *warm/cold colors*. The vector wind is overlaid only when the correlation between the TGF and 850 hPa wind is significant at the 0.05 level



typhoon activity is relatively inactive. It is evident that the TGF has both inter-annual and inter-decadal variability, but no significant trend in this period.

Table 1 lists the active/inactive TGF years defined as the standardized TGF index greater than 0.5/less than -0.5 standard deviation, and cold/warm events defined as Niño-3.4 index below/above 0.5 °C. It is evident that there are 15 active TGF years including 2 cold event and 5 warm events, 16 inactive TGF years with 6 cold events and 2 warm events, and 20 normal TGF years with 6 cold events and 4 warm events. As a result, there is no corresponding relationships between TGF active/inactive years and cold/warm events, which is consistent with previous studies (Chan 1985; Lander and Holland 1993; Ramage and Hori 1981; Wang and Chan 2002). This result also indicates that ENSO is not a major contributor to the variation of the TGF, though ENSO is the strongest inter-annual variability signal in tropical Pacific. However, this does not exclude that ENSO has no relation with the TGF. Indeed, there are significant correlations between the TGF and SST in central Pacific (Fig. 2b), with correlation above 0.28 (significant at the 0.05 level) between time series of the Niño-3.4 and JASO TGF indices. Since ENSO is not a major contributor to the variation of TGF,

next we explore the linkage between the TGF and SSTA in the whole Pacific.

4 Linking the TGF to spring SST predictors

As mentioned in the introduction, spring NPO may serve as a potential predictor for the frequency of TC formations over WNP (Chen et al. 2015; Fan 2007). Previous studies have suggested that the boreal wintertime NPO forces tropical Pacific SSTA in the following winter via the “seasonal footprinting mechanism (SFM)” (e.g., Vimont et al. 2001, 2003a, 2003b, 2009; Alexander et al. 2010). In addition, Zhan et al. (2013) suggested that boreal spring SST gradient (SSTG) between the Southwest Pacific and the Western Pacific warm pool might control the interannual variability of the TC frequency over the WNP. They found that the SSTG can explain 53% of the total WNP TC genesis frequency during the typhoon season for the period 1980–2011. However, we found that the Western Pacific Warm pool was not obviously correlated with the TGF, and the correlation between SSTG and TGF is only -0.46 in the 1980–2011 period, and -0.36 in the 1965–2016 period. Thus the index of SSTG might be related to the data

Table 1 Active, normal and inactive year based on the SD of the frequency of typhoon genesis. Cold events indicated with italic, and warm events with bold

Active (>0.5 SD)	1965, 1966, 1967, 1971, 1972, 1987, 1991 , 1992, 1993, 1994, 1995, 1996, 1997 , 2001, 2013
Normal (-0.5 to 0.5 SD)	1968, 1973, 1974, 1975, 1978, 1980, 1982 , 1984, 1985, 1986, 1989, 1990, 2000, 2003, 2004 , 2005, 2007, 2009 , 2012, 2015
Inactive (<0.5 SD)	1969, 1970, 1976, 1977, 1979, 1981, 1983, 1988, 1998, 1999, 2002, 2006 , 2008, 2010, 2011, 2014

Cold events indicated with italic, and warm events with bold

period and TC intensity. In addition, the anomalous SST in Tropical Pacific may be influenced by the North and South Pacific. Hence, it is hypothesized that the WNP TGF in JASO may be under the combined impact of the spring SST in North, Tropical and Southwest Pacific.

To investigate the influence of SST in the Pacific on the TGF, we first examine the correlations between the JASO TGF index and SSTA in preceding 7 months from Dec(-1), January to June and the JASO season, where Dec(-1) denote the December in the previous year (Fig. 3).

In the North Pacific, the distribution of the correlations mainly shows a prominent tri-polar pattern: two positive

correlation areas stretching to northwest (north branch) and southwest (south branch) of 30°N along the west coast of North America, and one zonal negative correlation area located from the tropical western Pacific to the central North Pacific.

This tri-polar pattern changes with seasons. In preceding 7 months (Dec(-1), Fig. 3a), the SST tri-polar correlation pattern is distinct, with larger values in the north branch between 40°–50°N of the North Pacific than in the south branch. In preceding 6 months (Jan, Fig. 3b), the tri-polar correlation pattern weakens. The SST in the south branch has almost no significant correlation with the TGF, while

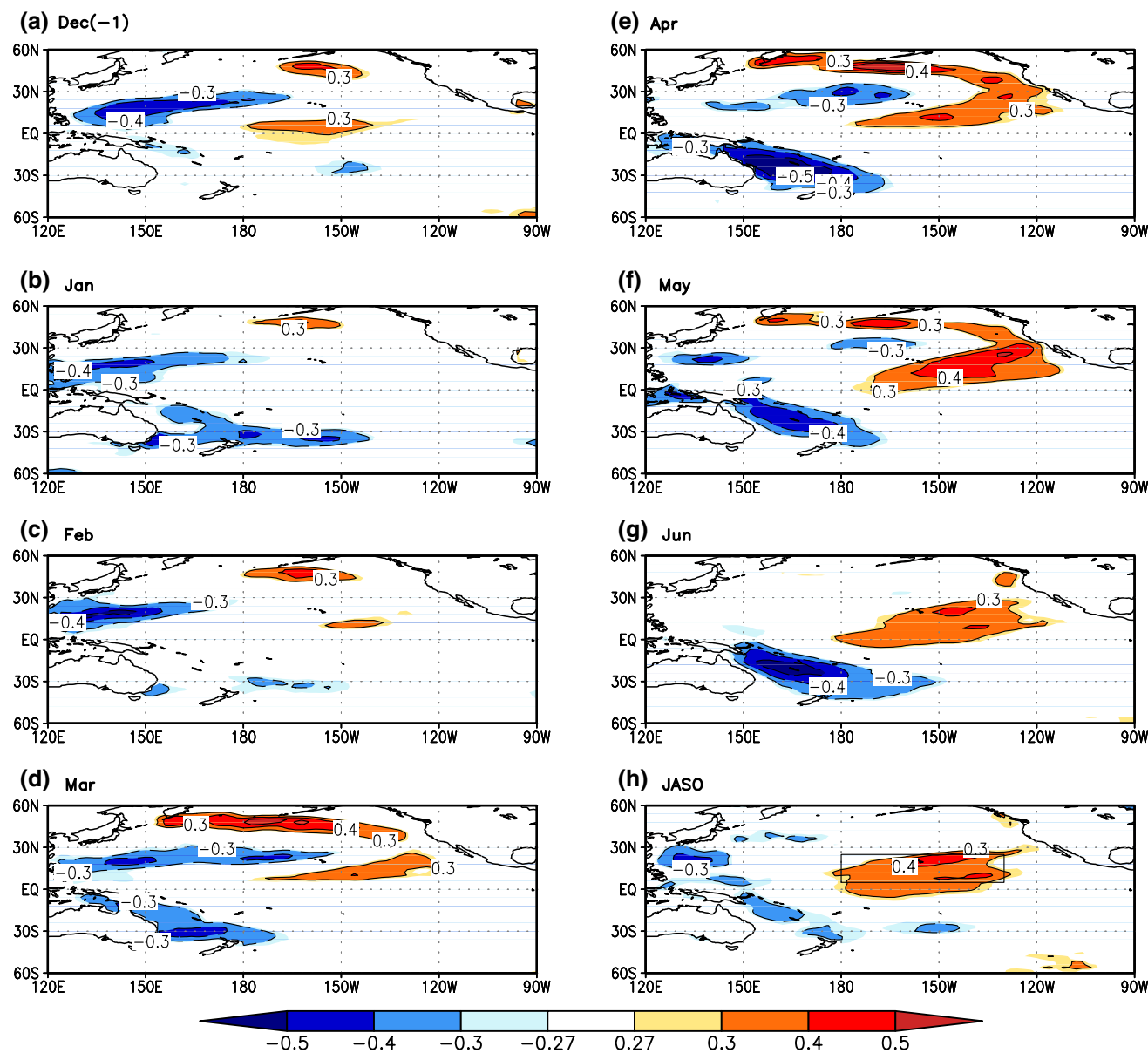


Fig. 3 Correlation between the JASO TGF index and SSTA in preceding December (Dec(-1)) (a), January (b), February (c), March (d), April (e), May (f), June (g) and JASO (h) in the 1965–2015

period. *Shading regions* are the correlation significant at the 0.05 level or below. The *black rectangular box* in g marked the approximate scope of significant region in JASO

SST in north branch is still stronger than the south branch. From February (Fig. 3c), SST in the south branch plays an increasing role to typhoon frequency. The tri-polar correlation pattern is well developed in March (Fig. 3d), and reaches the strongest in April (Fig. 3e). Two positive areas are connected near the west coast of North America, forming a semicircle and enveloping the zonal negative correlation region. The south branch of the semicircle stretches southwest across the dateline, and the centre of equatorial Pacific. From May to June, the tri-polar pattern in the North Pacific shifts: the north branch of 30°N tends to weaken and even disappear, the negative centre around the 30°N also weakens, while the strength and scope of the south branch keep increasing (Fig. 3f, g). In typhoon season (JASO), the significant positive correlations between the typhoon frequency and SST are concentrated in boxed region of (180°–130°W, 5°–25°N) (Fig. 3h), implying that warming SST in the centre of tropical North Pacific is favorable to the typhoon formation. Since the central tropical North Pacific covers the south branch of the tri-polar pattern, it is expected that the persistent increasing influence of SST in south branch (Fig. 3d–g) may to extend its influence into the typhoon season (JASO).

In addition to the tri-polar pattern in the North Pacific, it is noticed that there are significantly negative correlations between the JASO TGF and SST near the east coast of Australia in the South Pacific, and become most significant in April. Putting together, it is found that the TGF may be

linked to changes of a tri-polar pattern in North Pacific and a negatively correlated SSTA centered near the east coast of Australia. These significant correlation patterns are most pronounced in April. Thus, in this study, spring (April) SSTA in the Pacific are selected as potential predictor to forecast the WNP TGF in JASO.

For the ease of the discussion, we choose four boxed areas where the JASO TGF is significantly correlated with SSTA: A1 (156°–142°W, 8°–16°N), A2 (178°–150°W, 44°–52°N), B1(162°E–164°W, 22°–34°N) and B2 (154°–170°E, 18°–30°S) (Fig. 4). The SST averaged over each boxed area was denoted as SST_{A1} , SST_{A2} , SST_{B1} and SST_{B2} . Accordingly, the North Pacific tri-polar (NPT) index was defined as $NPT = SST_{A1} + SST_{A2} - SST_{B1}$, and the index of Coral Sea off the east coast of Australia as $CSST = SST_{B2}$.

Figure 5a, b show correlations between the JASO TGF and preceding monthly indices of NPT and $-CSST$, respectively. The maximum correlation happens in April with value of 0.56 and 0.57, both significantly at the 0.005 level. These results further support that NPT and CSST in April have strong links to the variation of frequency of typhoon genesis in the following typhoon season. As shown in Fig. 5c, d, both NPT and CSST in April have inter-decadal and inter-annual variability during the period of 1965–2015, consistent with the time series of the TGF (Fig. 2a). In addition, the April NPT has a decreasing trend with slope 0.0120°C/year, significant at the 0.1 level,

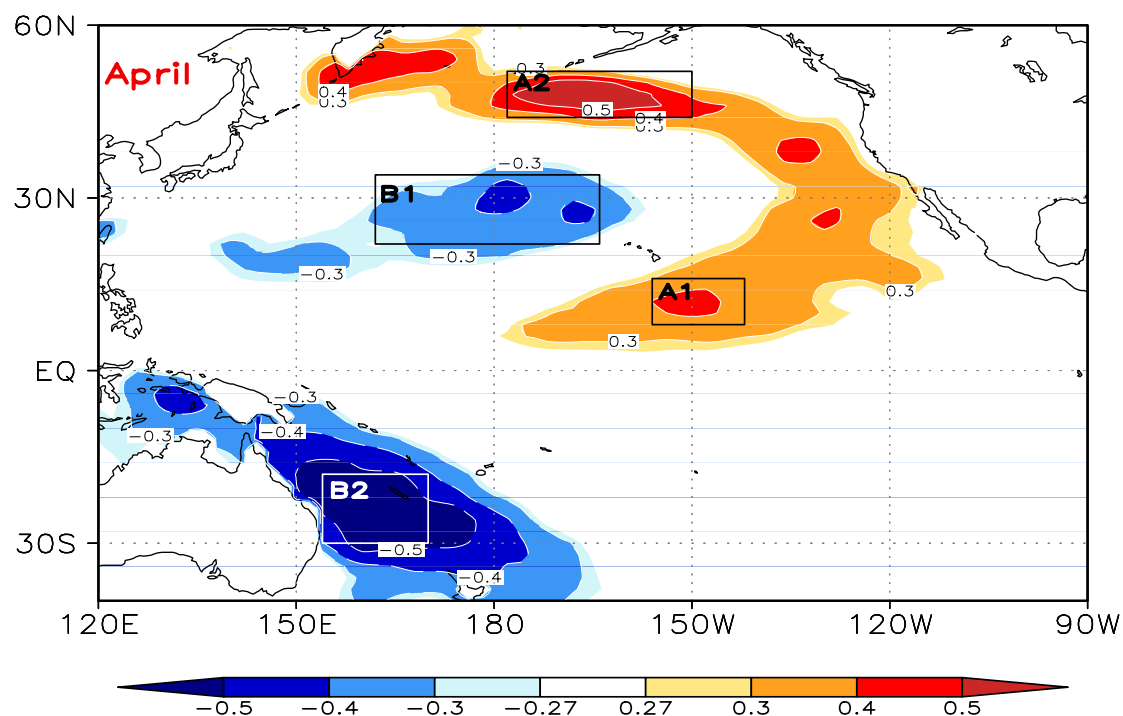
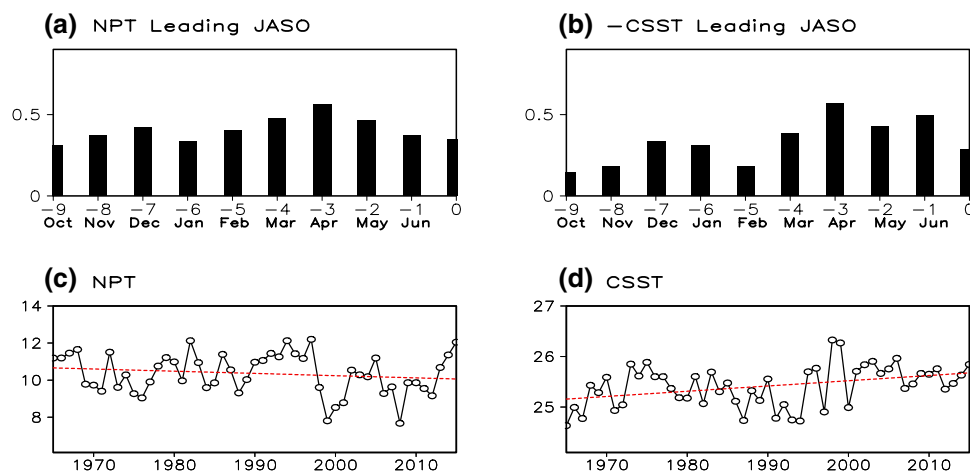


Fig. 4 Same as Fig. 3e, the *rectangular boxes* indicate the areas used to define April NPT and CSST index

Fig. 5 Monthly preceding correlation of NPT (a) and -CSST (b) with the frequency of typhoon in JASO over the Western North Pacific. Time series of April NPT (c) and CSST (d) index. The dotted line is trend line



while the April CSST has an increasing trend with slope $0.0103\text{ }^{\circ}\text{C}/\text{year}$, significant at the 0.05 level.

5 Possible mechanism of the identified spring SST predictors

We have demonstrated in Sect. 4 that correlations between the JASO TGF and April SSTA manifest as a tri-polar pattern (NPT_{Apr}) in the North Pacific and a large negative patch (CSST_{Apr}) off the east coast of Australia (Fig. 4). Therefore, NPT_{Apr} and CSST_{Apr} represent the SST variations that are better associated with the JASO TGF. But it is not clear how the influence of April NPT and CSST can last 3 months to the typhoon season (JASO). To address these questions, we first examine the seasonal evolution of NPT/CSST patterns and low-level wind anomalies from winter (D(-1)JFM) to the following typhoon season (JASO) by using partial correlations between NPT/CSST index and SSTA/850 hPa wind in the Pacific after linear removal of the ENSO effect (Figs. 6, 7). In previous winter and early spring (D(-1)JFM, Fig. 6a), a tri-polar SSTA pattern has formed in the North Pacific, which include a couple of positive SSTA branches and a negative band. The positive regions extend from the west coast of North America to Aleutian Islands and to the central tropical North Pacific, respectively. The negative region stretches from the subtropical Western Pacific to the central North Pacific. In the tropical Eastern Pacific, the SSTA is negative. Corresponding to the tri-polar SSTA pattern, anomalous cyclonic circulation almost controls the whole North Pacific, with the center over the east of Hawaiian Islands. On the south side of the cyclonic circulation, the anomalous southwesterly dominates the central tropical North Pacific, and along with west wind anomalies in tropical Western Pacific and east wind anomalies in tropical Eastern Pacific related to cold SSTA. In JFMA (Fig. 6b), the tri-polar SSTA of North

Pacific enhances obviously with the two positive SSTA bands joining together to a semicircle.

In response to the enhanced tri-polar SSTA, the cyclonic circulation near the Hawaiian Islands strengthens and expands in the North Pacific. In FMAM (Fig. 6c), this pattern gets the strongest. The anomalous southwesterly blows from east of Indonesia to the southern California coast. As a result, the northeasterly trade wind over the central tropical North Pacific weakens, leading to decreased evaporation and warming SST. We notice that the positive SSTA almost dominates the key region associated with TGF in typhoon season (indicated with black rectangular box), which increases the SST gradient between the both sides. The increased the SST gradient between western and central tropical North Pacific amplifies the westerly anomalies over the tropical North Pacific and makes its way to join the south side of cyclonic circulation.

Therefore, the abnormal westerly has two main effects: one is the warm pool preferring to expand eastward driven by westerly wind stress, the other is enhancing the abnormal westerly on the south side of cyclonic circulation, and weakening the evaporation of sea surface in the central tropical North Pacific. The two aspects sustain the warming of SST in the central tropical North Pacific, and act as positive feedback of air-sea interaction.

In the next few months (Fig. 6d), there are similar tri-polar patterns with intensity gradually weakened. With summer coming (AMJJ, Fig. 6e, f), the positive SSTA near the Aleutian becomes contracted, associated with easterly disappearance, and negative anomaly signals in tropical western Pacific weakens and even vanishes. Compared to Fig. 6a-d, the scope of the abnormal northerly over tropical western Pacific shrinks apparently for the establishment of southwest summer monsoon in Southeast Asia. The anomalous cyclonic circulation over the North Pacific is no longer complete, especially that north of 30°N weakens and even disappears. Thus, the

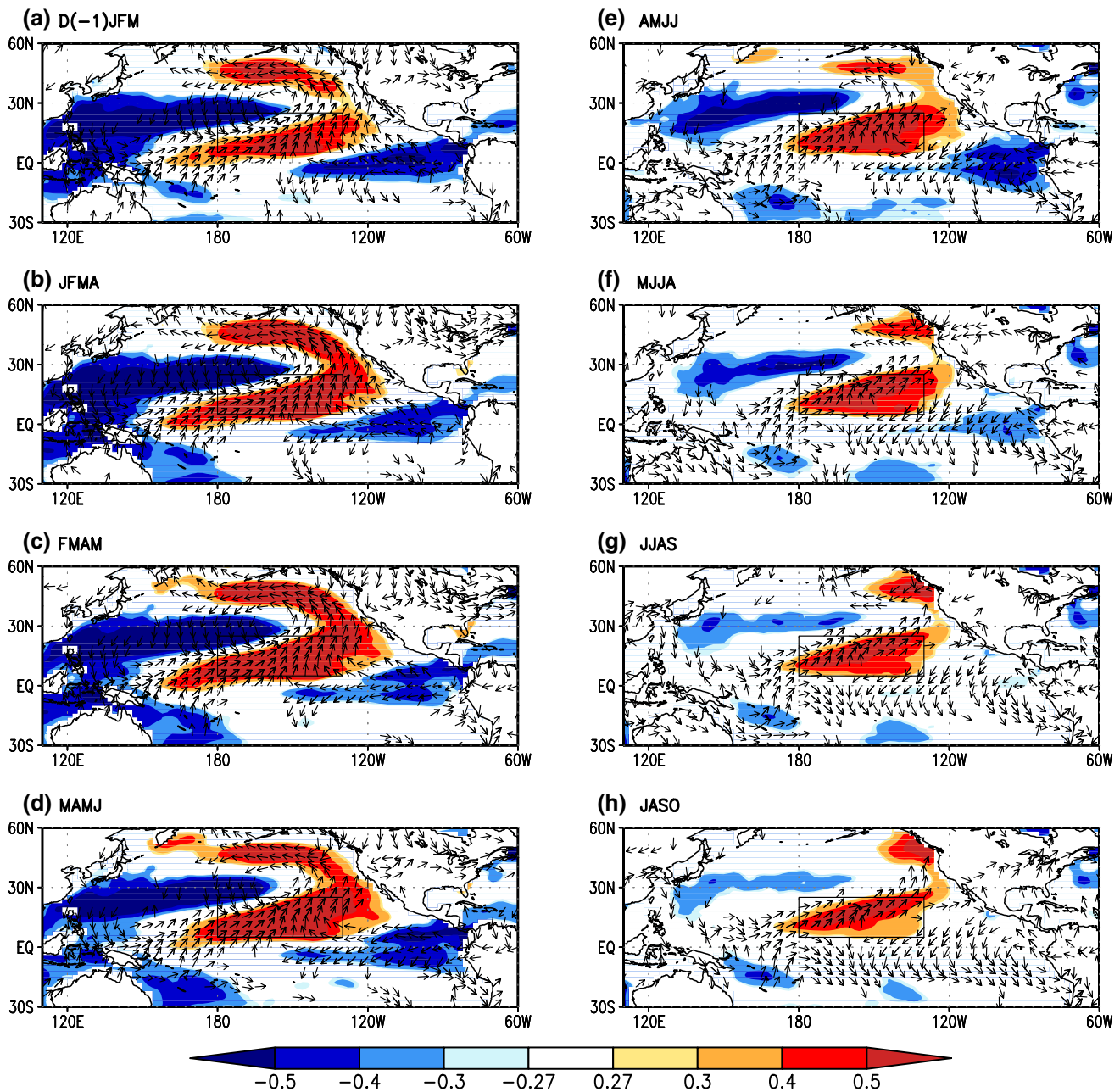


Fig. 6 Partial correlation between NPT index and SSTA / 850 hPa wind of every 4 months during the period 1965–2015 after removal of the ENSO effect in, **a** D(-1)JFM, **b** JFMA, **c** FMAM, **d** MAMJ, **e** AMJJ, **f** MJJA, **g** JJAS, **h** JASO. The red and blue shaded areas are positive and negative SSTA, respectively, and arrows denote the

wind, with correlation significant at the 0.05 level or below in all picture. The black rectangular box indicate the significant correlation area with typhoon frequency in typhoon season (same as Fig. 3h), and D(-1) means December of the previous year of the current year

tri-polar pattern of winter and spring has shifted. From summer to typhoon season (Fig. 6g, h), the south branch warming signals constantly control the central tropical North Pacific, and the SST gradient maintains between western and central tropical North Pacific. Therefore, the anomalous cyclonic curvature maintains over the west of dateline.

The above analysis suggests that the tri-polar patterns of SSTA signal over the North Pacific can last from previous winter to typhoon season, accompanying with abnormal cyclonic circulation, though their strength and scope change with the season. Especially, the abnormal warming signal (the south branch of tri-polar patterns) can last to typhoon season in the key region (Fig. 3h, noted by

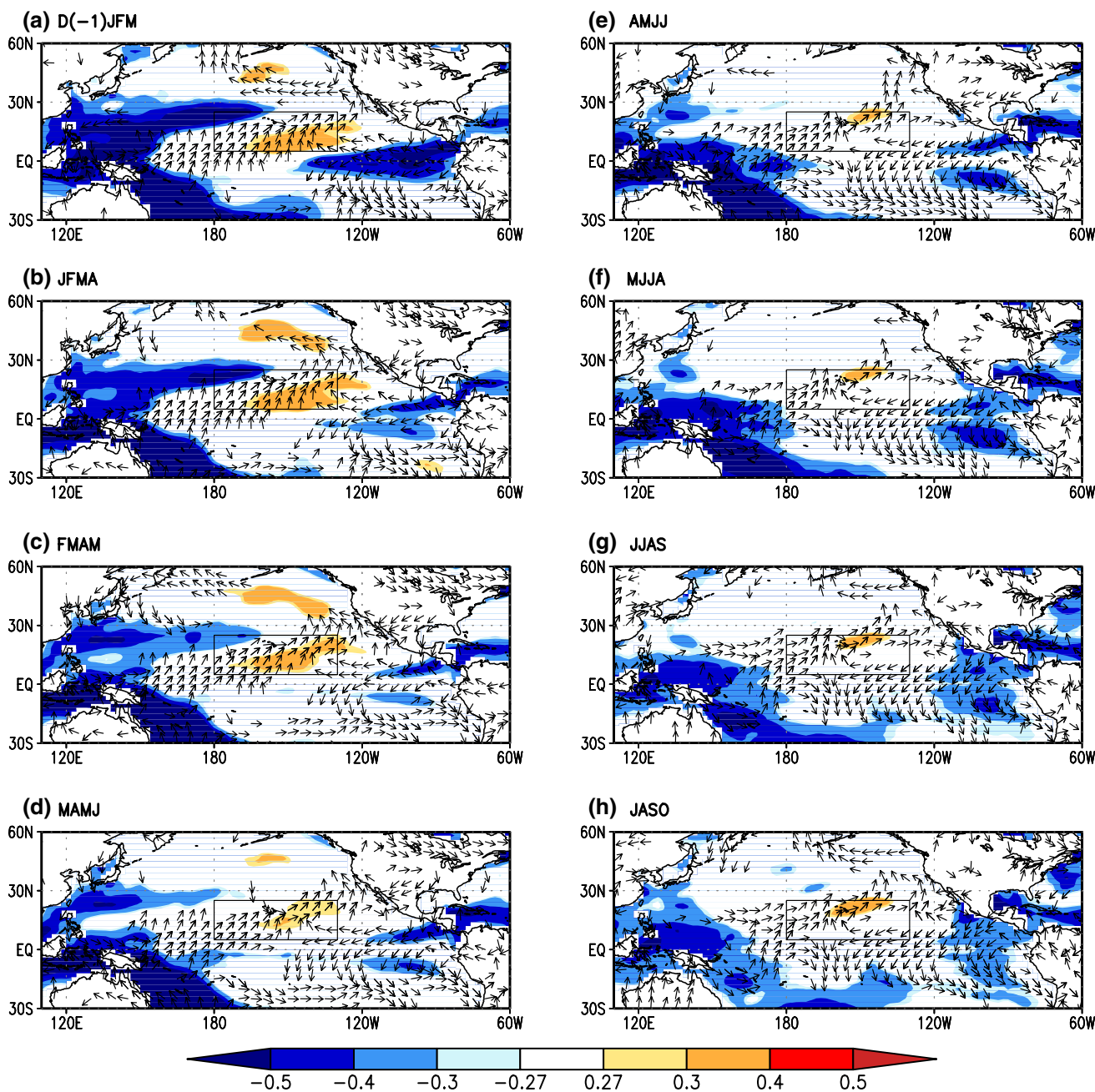


Fig. 7 Same as Fig. 6 but for $-CSST$

the black rectangular box), which is associated with the typhoon genesis frequency.

The low-level vorticity and the vertical zonal wind shear between upper and lower levels are the crucial environmental conditions for TC genesis and development (Gray 1968). The similar partial correlations (after removal of ENSO) between NPT_{Apr} index and relative vorticity at 850 hPa in JASO and between NPT_{Apr} index and vertical zonal wind shear between 200–850 hPa in JASO effect are displayed in Fig. 8. It's obvious that abnormal cyclonic vorticity almost

controls the west of dateline region (Fig. 8a), which is the major region for typhoon genesis. NPT_{Apr} has negative relationship with the vertical zonal wind shear of typhoon season over most of the tropical western and central Pacific region (Fig. 8b), that is, positive NPT_{Apr} is likely to weaken the vertical zonal wind shear. Previous studies showed that the situation with low vertical zonal wind shear was favorable for TC genesis and development, and vice versa (Zhou and Cui 2011; Liu and Chan 2013). Therefore, we conclude that positive NPT_{Apr} favors typhoon genesis.

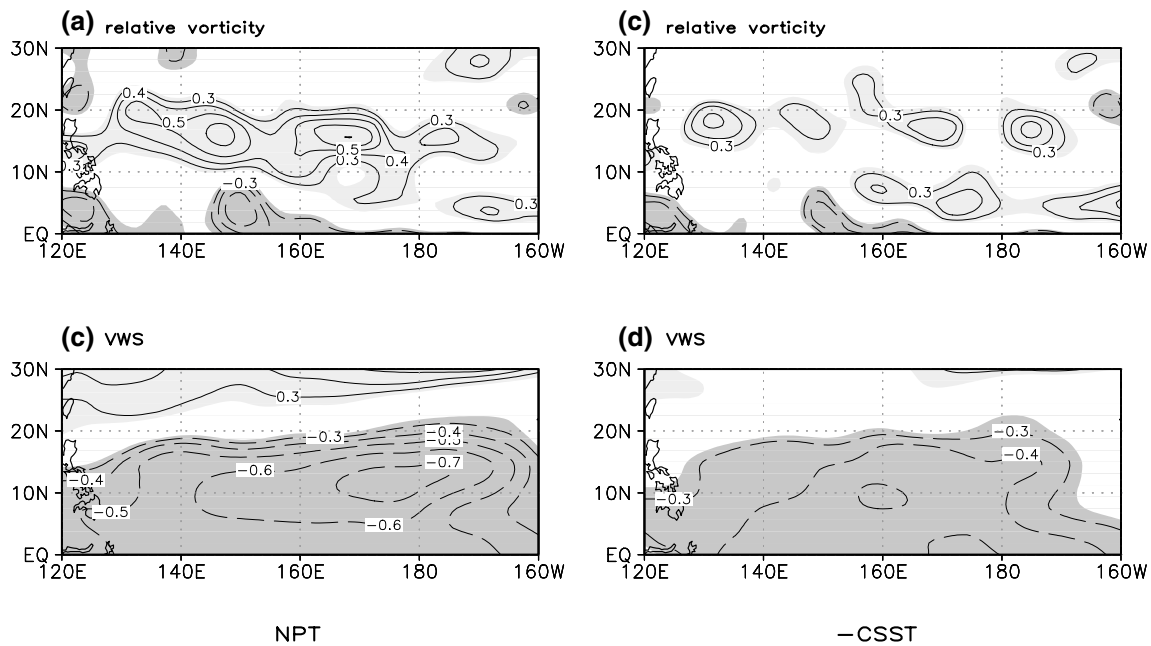


Fig. 8 Partial correlation **a** between NPT_{Apr} index and relative vorticity at 850 hPa in JASO, **b** between NPT_{Apr} index and vertical zonal wind shear of 200–850 hPa in JASO, **c** between $-CSST_{Apr}$ index and relative vorticity at 850 hPa in JASO, **d** between $-CSST_{Apr}$ index and

vertical zonal wind shear of 200–850 hPa in JASO during the period 1965–2015 after removal of the ENSO effect. The *light* and *dark shaded area* are positive and negative correlation significant at the 0.05 level or below in all picture

These results further confirm that the tri-polar pattern of SST in April induces anomalous low-level cyclonic circulation over the WNP, and this linkage has strong seasonal persistence and can last to the following JASO. Correspondingly, the vertical zonal wind shear weakens and positive low-level vorticity persists in the main region of typhoon genesis in JASO. The above conditions are favorable for the increase of TGF.

Similar analysis is done with April CSST index (Fig. 7). Considering that there is obvious inverse correlation between CSST and the frequency of typhoon, it would be convenient to use $-CSST$ rather than CSST. In previous winter to spring (D(-1)JFM-FMAM, Fig. 7a–c), the significant correlation area is concentrated between 30° poleward of the equator. The tri-polar pattern in the North Pacific is obviously weakened comparing with that of the NPT. Correspondingly, there is no complete cyclonic circulation over the North Pacific but consistent southwest wind prevailing from the west of Papua New Guinea (west of $150^\circ E$) to the south coast of California (northward to $30^\circ N$). Negative SSTA signals of east and north coast of Australia are significant and tend to maintain the temperature gradient between the central tropical North Pacific and west of dateline in south hemisphere. These also contribute to the development of the cross-equatorial Southern South westerly (SSW) anomalies over the west of data line. The negative SST anomalies in subtropical west Pacific and tropical eastern Pacific

shrink westward and eastward, respectively (Fig. 7d–f), and positive SSTA in the key region (noted by box in Fig. 7) associated with frequency of typhoon also continues to shrink and confine in 160° – $140^\circ W$ during the following MAMJ-MJJA. By contrast, the negative SSTAs along the east and north coast of Australia are still evident. The corresponding cross-equatorial SSW winds blows northeastward from north of Australia, across the equator, and to about $40^\circ N$. This pattern sustains through summer with weak intensity to typhoon season (Fig. 7f–h). It effectively reduces the northeast trade wind, and helps to keep warming in the centre of tropical North Pacific. The impact of westerly wind anomalies over 10° – $20^\circ N$ in the western Pacific on typhoon genesis is significant, providing favorable condition with cyclonic shear. Meanwhile, abnormal cyclonic vorticity and weakened vertical zonal wind shear occur in the following JASO over WNP (Fig. 8c, d). After typhoon season, the positive SSTA an abnormal westerly winds disappear (not shown).

The above results show that, the cyclonic wind anomaly in the tropical western Pacific and the SST in the tropical central North Pacific associated with NPT_{Apr} and $CSST_{Apr}$ are successive from previous winter to the typhoon season, forming favorite conditions for the typhoon formation over WNP.

In order to further examine these results, we classify the standardized NPT_{Apr} and $CSST_{Apr}$ indices into three

categories: strong (≥ 0.5 SD), neutrality (-0.5 to 0.5 SD) and weak (≤ -0.5 SD), and then combine them into nine categories. The years of each category are listed in Table 2.

The largest number of years among nine categories occurred in the combination of the strong NPT and weak CSST indices, 13 year in the period of 51 year (1965–2015), or around 25% of the total number of years. Among the 13 year, there are 11 years with active typhoon, namely, the probability of 85%. So, the most appropriate combination for typhoon genesis is strong NPT and weak CSST. The second most number is 8 year in the situation of weak NPT and neutral CSST indices, and the third is 7 year in the combination of weak NPT and strong CSST. They both exhibit an opposite situation to that of active typhoon years. The former has only 1 year active typhoon among the total number of 8 year, with the probability of 12.5%. The later also does not favor the typhoon genesis (2 year out of 7 year). Thus, when NPT is weak, accompanying with reversal sign or

small CSST index, the typhoon genesis is suppressed. There are no obvious differences in other 6 categories.

The composite circulation anomalies of the top 3 categories (Fig. 9) show that, in the situation of strong NPT and weak CSST, the positive anomaly of relative vorticity at 850 hPa, the negative anomaly of vertical wind shear between 200 and 850 hPa, and the positive anomaly of divergence at 200 hPa occur in the dominating region of typhoon genesis, which provide favorable and crucial environmental conditions for typhoon genesis. The opposite situation happen in the combinations of weak NPT and strong CSST, weak NPT and neutral CSST, which are adverse to typhoon genesis over the WNP.

In summary, our results illustrate that the variation of typhoon frequency over entire Western North Pacific is linked closely with the tri-polar pattern of SSTA distribution in North Pacific and negative SSTA in the coral sea of Australia in April.

Table 2 The list of the year with anomaly frequency of typhoon formation based on the nine combinations of the SD of April NPT and CSST index (the active typhoon years denoted by italics)

NTP	CSST		
	Strong (≥ 0.5)	Neutrality (-0.5 to 0.5)	Weak (≤ -0.5)
Strong (≥ 0.5)	1983, <i>1995, 1996, 2005</i> , 2014, <i>2015</i>	<i>1968, 1990</i>	<i>1965, 1966, 1967, 1972</i> , 1979, <i>1980, 1982</i> , 1986, <i>1991, 1992, 1993, 1994, 1997</i>
Neutrality (-0.5 to 0.5)	2002, <i>2003</i> , 2004, 2009, 2010	1974, 1977, <i>1978</i> , 1981, <i>1985, 2013</i>	<i>1987, 1989</i>
Weak (≤ -0.5)	<i>1973</i> , 1975, 1998, 1999, <i>2001</i> , 2006, 2011	1969, 1970, 1976, <i>1984</i> , 1988, 2007, 2008, 2012	<i>1971, 2000</i>

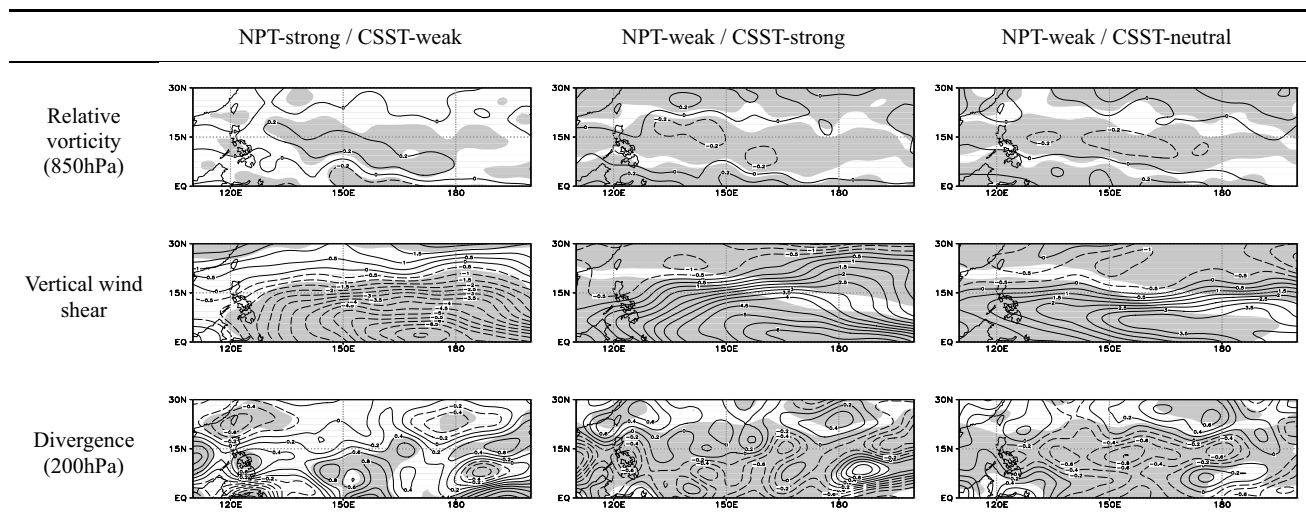


Fig. 9 The composite circulation anomalies in JASO of top three categories based on Table 2. Regions above the 95% significance level are shaded

6 Forecasting the TGF by Poisson regression

In this section, we aim to build a statistical model to forecast the TGF based on the identified two spring SST predictors (NPT_{Apr} and $CSST_{Apr}$). As the TGF is a count variable for the typhoon (rare) events, it is natural to use Poisson regression. Poisson regression assumes the response variable has a Poisson distribution, and assumes the logarithm of its expected value can be modeled by a linear combination of unknown predictors. To proceed, we need demonstrate that the distribution of the response variable Y (i.e., the JASO TGF) taken integer values $y = 0, 1, 2, \dots$ follows a Poisson distribution with parameter λ with probability

$$P\{Y = y\} = \frac{e^{-\lambda} \lambda^y}{y!} \tag{1}$$

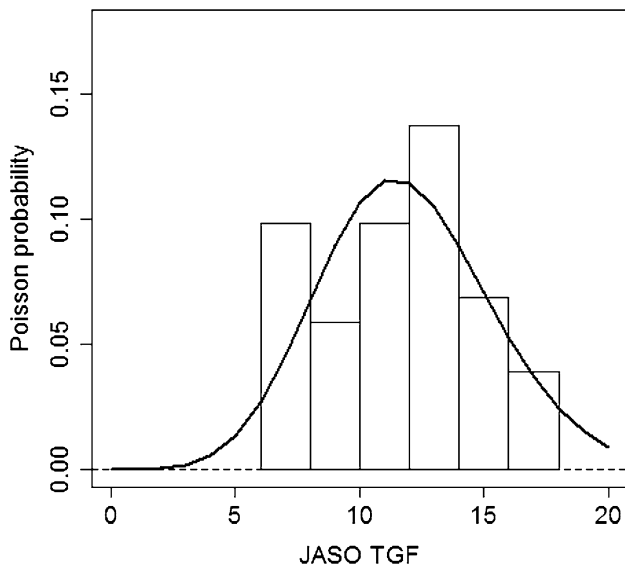


Fig. 10 Histogram and estimated Poisson probability function (with parameter $\lambda = 11.86$) for JASO TGF in 1965–2015

Table 3 Parameter estimates (\pm SE) and p-values (bold values indicate significance at the 0.05 level) of the likelihood ratio test for the Poisson models, with and without predictors X_{1t} and X_{2t} in PM-I and PM-II (in the first and second rows), where $t = 1, 2, \dots, n$ denotes the

Poisson models	Mean TGF $\lambda(X_{1t}, X_{2t})$	AIC	p value	R^2
PM-I $NPT_{Apr}(X_{1t})$	$\exp(1.10 + 0.13X_{1t})$ $\pm 0.41 \pm 0.04$	248.36	0.0006	0.32
PM-II $CSST_{Apr}(X_{2t})$	$\exp(11.22 - 0.34X_{2t})$ $\pm 2.55 \pm 0.10$	248.44	0.00058	0.33
PM-III (X_{1t} and X_{2t})	$\exp(7.61 + 0.09X_{1t} - 0.24X_{2t})$ $\pm 3.03 \pm 0.04 \pm 0.11$	245.67	0.029 (0.03)	0.45

As shown in Fig. 10, the JASO TGF follows a fitted Poisson with parameter $\lambda = 11.86$. Thus, Poisson regression approach could be used to model the relationship between the TGF and two identified predictors NPT_{Apr} and $CSST_{Apr}$ by allowing the parameter λ depending on predictors.

Mathematically, given input predictors X_{1t} and X_{2t} (i.e., NPT_{Apr} and $CSST_{Apr}$) and their observed values (x_{1t}, x_{2t}) for $t = 1, 2, \dots, n$, we notice that Poisson parameter $\lambda = \lambda(x_{1t}, x_{2t})$ is the mean response Y , and yield,

$$\lambda = \lambda(x_{1t}, x_{2t}) = E(Y|X_1 = x_{1t}, X_2 = x_{2t}) = \exp(\alpha + \beta_1 x_{1t} + \beta_2 x_{2t}) \tag{2}$$

To estimate parameters $(\alpha, \beta_1, \beta_2)$, we applied a generalized linear model (GLM) framework in the Poisson model. By doing so, the statistical significance of predictor effect on Poisson parameter $\lambda = \lambda(X_{1t}, X_{2t})$ can be evaluated based on the likelihood ratio test based on the observed data (x_{1t}, x_{2t}) for $t = 1, 2, \dots, n$. Table 3 contains parameter estimates along with standard errors and p-values of the likelihood tests, which indicate significant predictors if smaller than a certain value, usually 5% for three Poisson models with predictors X_{1t} , X_{2t} and both fitted to the parameter λ . As indicated in the table, X_{1t} and X_{2t} (i.e., NPT_{Apr} and $CSST_{Apr}$) are highly significant in the associated Poisson models PM-I to PM-III, respectively. In particular, PM-III with both NPT_{Apr} and $CSST_{Apr}$ as predictors has the smallest AIC value 245.67, implying that the PM-III is most appropriate to be selected as a predictive model for the JASO TGF, compared to other two single predictor Poisson models PM-I and PM-II. This predictive model based on NPT_{Apr} and $CSST_{Apr}$ can capture 45% variance of the JASO TGF during the 1965–2015 period.

In order to further demonstrate that the forecasting skill of Poisson regression approach based on two predictors NPT_{Apr} and $CSST_{Apr}$, a separate model was derived using the observed data over the training period 1965–1998. The predictive values after 1998 therefore indicate the true skill of this approach. Specifically, by applying the training data

year in the record period; p value 0.029(0.03) in the third row is of likelihood ratio test for the Poisson model PM-III versus PM-I and PM-II, respectively

in the 1965–1998 period ($n = 34$), we have the fitted Poisson regression model

$$\hat{\lambda}(X_{1t}, X_{2t}) = \exp(6.7 + 0.10X_{1t} - 0.21X_{2t}). \quad (3)$$

Note that the model in Eq. (3) based on the training data in 1965–1998 is slightly different from PM-III in Table 3 using the whole data in 1965–2015. Thus, the JASO TGF can be estimated by $\exp(6.7 + 0.10NPT_{APR} - 0.21CSST_{APR})$.

Figure 11 demonstrates this skill by showing the associated correlation coefficients and the root mean square error (RMSE) in both training and testing periods. In general, the performance of model (3) evident in the training period is maintaining during the subsequent testing period. The correlation coefficient between the predicted and observed values of the TGF is 0.65 for the training period 1965–1998 (noted by Cor_0), and the corresponding RMSE is 2.21 (noted by $RMSE_0$). The correlation coefficient between the predicted and observed numbers of typhoon formation over WNP is 0.52 for period of 1996–2015 (noted by Cor_1), and the corresponding RMSE is 2.0544 (noted by $RMSE_1$). These results suggest that the skill observed in the training period also maintains in the testing period. In particular, the performance of forecasting skill in last 4 years (2012–2015) is notable with close forecasted TGF values to observed

ones, except overestimating TGF in 2014 when the season's peak months August and September saw a very low to no activity of tropical cyclones caused by an unusually strong and a persistent suppressing phase of the Madden-Julian Oscillation (MJO) (Lea and Saunders 2015). Therefore, the spring (April) NPT and CSST indices may provide a reasonably well skill to forecast the frequency of typhoon genesis through the Poisson regression approach.

7 Conclusion and discussion

In this work, the predictability of the JASO TGF and associated boreal spring (April) SST in the Pacific has been investigated. It is found that, the JASO TGF is positively related to a tri-polar pattern of SSTA in April of North Pacific (NPT_{Apr}), while it negatively related to SSTA over the Coral Sea ($CSST_{Apr}$) off east Australia coast. The possible physical mechanism is also discussed without considering the impact of ENSO. During previous winter and spring, the NPT pattern is characterized by the SST positive anomalies along the west coast of North America stretching to northwest Pacific and to tropical central-Pacific, north of the equator, respectively. It forms a semi-circle to envelop the negative anomalies of the central North Pacific. Complying with NPT pattern, a strong and large cyclonic anomaly circulation dominates over the North Pacific, and wide abnormal westerly from its bottom blows from western to the central tropical north Pacific. Abnormal westerly weakens the prevailing northeasterly trade wind, leading to decreased evaporation and warming SST in the central tropical north Pacific. Abnormal westerly wind stress in western Pacific may stimulate the water of warm pool to expand to the central Pacific and result in warming in the central Pacific. However, the warming effect occurs only in the ocean to the north of the equator, because of the cold SSTA on the Coral Sea ($CSST$) off the east coast of Australia. The meridional circulation is enhanced for increasing temperature gradient between the central tropical north Pacific and east-north coast of Australia. The abnormal Southern south westerly cross-equatorial flow blows from the southern hemisphere (near Australia) across through equator to the central tropical north Pacific. This flow plays an essential role in two aspects, one strengthening zonal westerly anomaly for the cross-equatorial flows get to equator then turn eastward to join the westerly in tropical western Pacific and the other to weaken the prevailing easterly trade wind, reduce evaporation, and result in continuous warming in the centre of tropical north Pacific and preventing abnormal warm region from expanding to southern hemisphere. From early summer to typhoon season, SST abnormal signal becomes weak for “reemergence mechanism” (Alexander et al. 1999), and the corresponding abnormal cyclonic

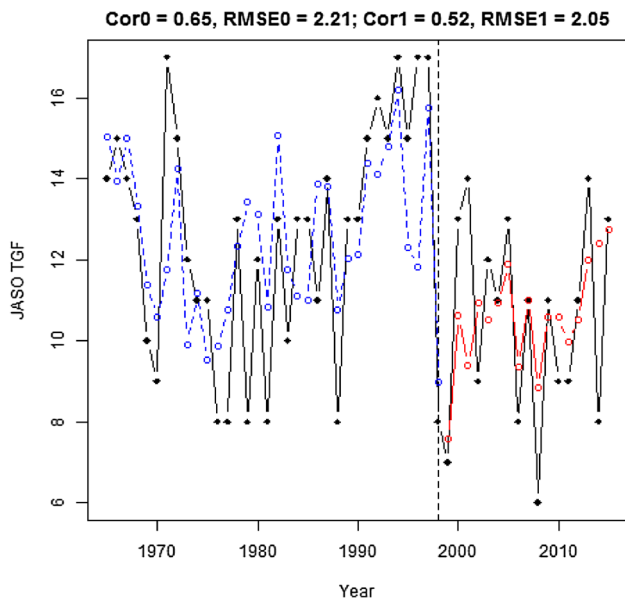


Fig. 11 Passion regression model results for forecasting the JASO TGF based on April NPT and CSST indices. The *solid line with filled circle* is the observed time series of the JASO TGF. *Blue dashed line with blue circles* are the model forecast of JASO TGF in the training period 1965–1998 and *red dashed line and circles* are the model forecasted value of JASO TGF in the testing period 1999–2015. Cor_0 and $RMSE_0$ are the correlation and root mean square error between observed and forecasted values in the training period and Cor_1 and $RMSE_1$ are the results for the testing period

Table 4 Correlations and partial correlations of NPT and CSST with TGF during 1965–2015

	SSTG	EASST	NPT	NPT SSTG	NPT EASST	CSST	CSST SSTG	CSST EASST
TGF	−0.36*	−0.47*	0.56*	–	–	−0.57*	–	–
NPT	0.20	−0.35*	–	–	–	–	–	–
CSST	0.65*	0.80*	–	–	–	–	–	–
TGF SSTG	–	–	–	0.54*	–	–	−0.48*	–
TGF EASST	–	–	–	–	0.48*	–	–	−0.36*

Here “X|Y” means the residuals of after linearly removing the effect of Y, where X and Y denote any variables listed in the table

*Significant at the 0.01 level

circulation over WNP also gets weak, but warming SST signal maintain in the centre of tropical north Pacific with southwest wind anomalies, which increases the horizontal temperature gradients between the west and the centre of tropical north Pacific, maintains abnormal cyclonic wind over ocean to the west of dateline, leads to cyclonic convergence over the major region of typhoon genesis, and forms favorite condition for typhoon genesis.

Observing that previous studies (Zhan et al. 2013; Zhou and Cui 2011) have studied the impact of the SST anomalies over the Coral Sea off east Australia coast (EASST) on TC genesis, to justify our findings on the relationship between the JASO TGF and NPT_{Apr} and $CSST_{Apr}$, we need discuss (1) the difference between the SSTG (Zhan et al. 2013) and EASST (Zhou and Cui 2011) and the spring NPT and CSST in this study; (2) the influence of SSTG and EASST on the relationship between the JASO TGF and NPT_{Apr} and $CSST_{Apr}$, respectively. To this end, we have calculated SSTG and EASST indices for the 1965–2015 period following Zhan et al. (2013) and Zhou and Cui (2011). As shown in Table 4, the correlation between the TGF and SSTG indices is -0.36 , which much lower than that of NPT ($Cor=0.56$) and CSST ($Cor = -0.57$). On other hand, Zhan et al. (2013) suggested that the SSTG could explain 53% variance (i.e., Correlation = -0.73) of TC during the 1980–2011 period, yet we find that the correlation between SSTG and TGF is only -0.46 in this period. As a result, our results indicate that NPT_{Apr} and $CSST_{Apr}$ are superior to the SSTG for capturing the variance of the typhoon genesis. Furthermore, since there is no significant correlation between spring NPT and SSTG, partial correlation between the TGF and NPT remains almost unchanged by comparing the original correlation (0.56) to the partial correlation (0.54) after removing the effect of the SSTG, implying that the TGF-NPT relation is independent of the influence of SSTG (Table 4). In contrast, the EASST dose have influence on the TGF-NPT relation as showing that the partial correlation is decreased from the original 0.56 to 0.48 after removing the effect of the EASST. For the influence of the SSTG/EASST on the TGF-CSST relation, since the SSTG and EASST are highly correlated to the CSST

with correlations 0.65 and 0.80 due to these indices were calculated using spring SST over some areas (e.g., the Coral Sea off east Australia coast) in the Southwest Pacific Ocean. However, the TGF-CSST relationship is largely independent of the influence of SSTG and EASST because the partial correlations (-0.48 and -0.36) between the TGF and CSST remains statistically significant at the 0.05 level by removing the effect of SSTG and EASST, respectively. The results indicate that NPT_{Apr} and $CSST_{Apr}$ have stronger relations to the TGF, compared to the SSTG and EASST which are linked to the TC genesis frequency. Therefore, NPT_{Apr} and $CSST_{Apr}$ may be used to forecast the TGF. In this study, we have demonstrated a Poisson regression model using NPT_{Apr} and $CSST_{Apr}$ can be devolved to predict the TGF and a promising skill is achieved. Finally, we give a discussion on the ENSO influence on the TGF. We have found that there are no corresponding relationships between TGF active/inactive years and cold/warm events (Table 1), which is consistent with previous studies (Chan 1985; Lander and Holland 1993; Ramage and Hori 1981; Wang and Chan 2002). However, the impact of ENSO on the TGF over WNP is rather complicated. Many studies showed that the relationship between ENSO and TGF existent, to a great extent, on the ENSO warming pattern. Zhang et al. (2015) pointed out that intense typhoon occurred more frequently over the WNP in the autumns of the CP El Niño than that of EP El Niño. Chen and Tam (2010) mentioned that TC occurrence was enhanced in most domains of the WNP during El Niño Modoki years. As the Niño-3.4 index was used in this study, it may include both CP and EP warmings, and so the partial correlation analysis with the Niño-3.4 index may not distinguish the respective influences of two types of ENSO. In the future studies, the different effects from the two type of ENSO should be taken into account in TGF prediction.

Acknowledgements This study is jointly supported by the Ministry of Science and Technology of China (Grant No. 2016YFA0601801), the National Natural Science Foundation of China (Grant Nos. 41575052, 41205066, 91437216, 41575075 and 91637312), the China Special Fund for Meteorological Research in the Public Interest (No. GYHY201406018), and a Project Funded by the Priority Academic

Program Development (PAPD) of Jiangsu Higher Education Institutions. Shanshan Zhong received support from China Scholarship Council under the visiting scholar program for conducting research at CSIRO in Australia.

References

- Alexander MA, Deser C, Timlin MS (1999) The reemergence of SST anomalies in the North Pacific Ocean. *J Clim* 12:2419–2433
- Alexander MA, Vimont DJ, Chang P, Scott JD (2010) The impact of extratropical atmospheric variability on ENSO: Testing the seasonal footprinting mechanism using coupled model experiments. *J Clim* 23:2885–2901
- Cameron AC, Trivedi PK (1998) Regression analysis of count data, 2nd edn. Cambridge University Press, New York, p 587
- Chan JCL (1985) Tropical cyclone activity in the northwest Pacific in relation to the El Niño /southern oscillation phenomenon. *Mon Wea Rev* 113:599–606
- Chan JCL (1995) Tropical cyclone activity in the Western North Pacific in relation to the stratospheric quasi-biennial oscillation. *Mon Wea Rev* 123:2567–2571
- Chan JCL (2000) Tropical cyclone activity over the western North Pacific associated with El Niño and La Niña events. *J Clim* 13:2960–2972. doi:10.1175/1520-0442(2000)013<2960>2.0.CO;2
- Chan JCL, Shi J, Lam CM (1998) Seasonal forecasting of tropical cyclone activity over the Western North Pacific and the South China Sea. *Wea Forecasting* 13:997–1004. doi:10.1175/1520-0434(1998)013<0997:SFOTCA>2.0.CO;2
- Chan JCL, Shi J, Lam CM (2001) Improvements in the seasonal casting of tropical cyclone activity over the western North Pacific. *Wea Forecast* 16:491–498
- Chand SS, Walsh KJE (2010) The influence of the Madden–Julian oscillation on tropical cyclone activity in the Fiji region. *J Clim* 23:868–886. doi:10.1175/2009JCLI3316.1
- Chen GH, Tam CY (2010) Different impacts of two kinds of Pacific Ocean warming on tropical cyclone frequency over the western North Pacific. *J Geophys Res Lett* 37:L01803. doi:10.1029/2009GL041708
- Chen TC, Weng SP, Yamazaki N, Kiehne S (1998) Interannual variation in the tropical cyclone formation over the western North Pacific. *Mon Wea Rev* 126:1080–1090
- Chen D, Wang H, Liu J, Li G (2015) Why the spring North Pacific Oscillation is a predictor of typhoon activity over the Western North Pacific. *Int J Climatol* 35:3353–3361. doi:10.1002/joc.4213
- Chia HH, Ropelewski CF (2002) The interannual variability in the Genesis location of tropical cyclone in the Northwest Pacific. *J Clim* 15:2934–2944. doi:10.1175/1520-0442(2002)015<2934:TIVITG>2.0.CO;2
- Dong K (1988) El Niño and tropical cyclone frequency in the Australian region and the northwest Pacific. *Aust Meteor Mag* 36:219–225
- Fan K (2007) New predictors and a new prediction model for the typhoon frequency over western North Pacific. *Sci China Ser (D)* 50:1417–1423
- Graham NE, Barnett TP (1987) Sea surface temperature, surface wind divergence, and convection over tropical oceans. *Science* 238:657–659
- Gray WM (1968) Global view of the origin of tropical disturbances and storms. *Mon Wea Rev* 96:669–700
- Gray WM (1979) Tropical cyclone intensity determination through upper-troposphere aircraft reconnaissance. *Bull Amer Meteor Soc* 60:1069–1074
- Gray WM (1984) Atlantic seasonal hurricane frequency. Part I: El Niño and 30mb quasi-biennial oscillation influences. *Mon Wea Rev* 112:1649–1668. doi:10.1175/1520-0493(1984)112<1649:ASHFPI>2.0.CO;2
- Kalnay E et al (1996) The NCEP/NCAR 40-year reanalysis project. *Bull Am Meteor Soc* 77:437–471. doi:10.1175/1520-0477(1996)077<0437:TNYRP.2.0.CO;2
- Lander MA (1994) An exploratory analysis of the relationship between tropical storm formation in the western north pacific and ENSO. *Mon Wea Rev* 122:636–651
- Lander M, Holland GJ (1993) On the interaction of tropical cyclone-scale vortices. I. *Quart. J R Meteor Soc* 119:1347–1361
- Lea A, Saunders M (2015) Summary of 2014 NW Pacific typhoon season and verification of authors' seasonal forecasts. *The Tropical Storm Risk*. Issued: 27th January 2015
- Li Y, Smith I (2009) A statistical downscaling model for Southern Australia Winter Rainfall. *J Clim* 22:1142–1158
- Li RCY, Zhou W (2012) Changes in Western Pacific tropical cyclones associated with the El Niño–Southern oscillation cycle. *J Clim* 25:5864–5878. doi:10.1175/JCLI-D-11-00430.1
- Li RCY, Zhou W (2013a) Modulation of Western North Pacific tropical cyclone activities by the ISO. Part 1: Genesis and intensity. *J Clim* 26:2904–2918
- Li RCY, Zhou W (2013b) Modulation of Western North Pacific tropical cyclone activities by the ISO. Part 2: Tracks and landfalls. *J Clim* 26:2919–2930
- Li RCY, Zhou W (2014) Interdecadal change in South China Sea tropical cyclone frequency in association with zonal sea surface temperature gradient. *J Clim* 27:5468–5480
- Li RCY, Zhou W (2015) Interdecadal changes in summertime tropical cyclone precipitation over Southeast China during 1960–2009. *J Clim* 28:1494–1509. doi:10.1175/JCLI-D-14-00246.1
- Li RCY, Zhou W, Chan JCL, Huang P (2012) Asymmetric modulation of the Western North Pacific cyclogenesis by the Madden–Julian Oscillation under ENSO conditions. *J Clim* 25:5374–5385. doi:10.1175/JCLI-D-11-00337.1
- Li X, Yu J, Li Y (2013) Recent summer rainfall increase and surface cooling over Northern Australia: A response to warming in the tropical Western Pacific. *J Clim* 26:7221–7239
- Liu KS, Chan JCL (2013) Inactive period of Western North Pacific tropical cyclone activity in 1998–2011. *J Clim* 26:2614–2630. doi:10.1175/JCLI-D-12-00053.1
- Ramage CS, Hori AM (1981) Meteorological aspects of El Niño. *Mon Wea Rev* 109:1827–1835. doi:10.1175/1520-0493(1981)109<1827:MAOEN>2.0.CO;2
- Simpson RH (1974) The hurricane disaster potential scale. *Weatherwise* 27:169–186
- Smith TM, Reynolds RW (2004) Improved Extended Reconstruction of SST (1854–1997). *J Clim* 17:2466–2477
- Vimont DJ, Battisti DS, Hirst AC (2001) Footprinting: A seasonal connection between the tropics and mid-latitudes. *Geophys Res Lett* 28:3923–3926
- Vimont DJ, Wallace JM, Battisti DS (2003a) The seasonal footprinting mechanism in the Pacific: Implications for ENSO. *J Clim* 16:2668–2675
- Vimont DJ, Battisti DS, Hirst AC (2003b) The seasonal footprinting mechanism in the CSIRO general circulation models. *J Clim* 16:2653–2667
- Vimont DJ, Alexander M, Fontaine A (2009) Midlatitude excitation of Tropical variability in the Pacific: The Role of thermodynamic coupling and seasonality. *J Clim* 22:518–534
- Wang B, Chan JCL (2002) How strong ENSO events affect tropical storm activity over the Western North Pacific. *J Clim* 15:1643–1658. doi:10.1175/1520-0442(2002)015<1643:HSEET>2.0.CO;2

- Wu ZW, Dou J, Lin H (2015) Potential influence of the november–december southern hemisphere annular mode on the East Asian winter precipitation: a new mechanism. *Clim Dyn* 44:1215–1226
- Yumoto M, Matsuura T (2001) Interdecadal variability of tropical cyclone activity in the Western North Pacific. *J Meteor Soc Japan* 79:23–35
- Zhan R, Wang Y (2016) CFSv2-based statistical prediction for seasonal accumulated cyclone energy (ACE) over the Western North Pacific. *J Climate* 29(2):525–541
- Zhan R, Wang Y, Wen M (2013) The SST gradient between the southwestern Pacific and the western Pacific warm pool: A new factor controlling the northwestern Pacific tropical cyclone genesis frequency. *J Clim* 26:2408–2415. doi:[10.1175/JCLI-D-12-00798.1](https://doi.org/10.1175/JCLI-D-12-00798.1)
- Zhang W, Leung Y, Fraedrich K (2015) Different El Niño types and intense typhoons in the Western North Pacific. *Clim Dyn* 44:2965–2977
- Zhou BT, Cui X (2011) Sea surface temperature east of Australia: a predictor of tropical cyclone frequency over the western North Pacific? *Chin Sci Bull* 56:196–201